

# The effects of air pollution on cultural heritage: The case study of Santa Maria delle Grazie al Naviglio Grande (Milan)\*

Valeria Comite<sup>a</sup> and Paola Fermo

Department of Chemistry, University of Milan, Via Golgi 19, 20133, Milan, Italy

Received: 10 July 2018 / Revised: 1 October 2018

Published online: 31 December 2018

© Società Italiana di Fisica / Springer-Verlag GmbH Germany, part of Springer Nature, 2018

**Abstract.** Atmospheric pollution causes monuments surface degradation in urban environments. Among the degradation processes the formation of black crusts (BCs) is one of the most dangerous phenomenon. During this process, aerosol particulate matter (PM) can be embedded into gypsum, one of the main crusts constituents, providing the characteristic black colour. EC (elemental carbon) and OC (organic carbon) are the responsible for the yellowing and blackening processes occurring on the surfaces and their quantification in the crusts can provide information on the contribution of atmospheric pollution sources to the degradation products formation. This research study is focused on the characterization of BCs collected from the Church of Santa Maria delle Grazie al Naviglio Grande in Milan, from the point of view of the effects of atmospheric pollution on cultural heritage. The analysed samples consist of mortars and bricks partially degraded and covered with black crusts. Applying different analytical techniques, such as FT-IR/ATR, CHN, TGA and IC, the crusts composition has been investigated focusing on the quantification of the carbonaceous fraction. This integrated approach has allowed to identify the sources of pollution responsible for the decay of the different building materials of the church.

## 1 Introduction

As is well known air pollution has negative effects on human health and climate change but also can induce damage on cultural heritage. The increasing urban pollution has been influenced over the centuries by the change of fuels (wood, coal, petroleum derivatives) that have released large amounts of sulfur dioxide (SO<sub>2</sub>), carbon monoxide (CO) and heavy metals into the air. These pollutants, together with carbon dioxide (CO<sub>2</sub>), nitrogen monoxide (NO) and unburnt hydrocarbons are the main causes of the deterioration of the surfaces of the monuments [1, 2].

Deterioration is an irreversible and inevitable phenomenon and speed and modes where it occurs depends on the type of material, the surrounding environment and also from the chemical-physical processes involved. Water, soluble salts and atmospheric pollutants, such as carbonaceous particles and metals, are deposited on the surfaces by dry or wet processes and are the responsible for the degradation.

The action of pollutants on the surface forms dark deposits called black crusts [1, 3–5] mainly present in areas protected from washout and exposed to polluting weathering agents [6–16]. Over time they determine the degradation of the substrate until complete pulverization.

The urban area of Milan is the most industrialized and densely populated city in Northern Italy with aerosols that often exceed the limits set by the directive on air quality (D. Lgs. 155/2010) [17]. Its position, in the middle of the Po Valley, leads to limited rainy events and winds generally tend to be weak or absent. The city of Milan suffers from high pollution produced by the intense vehicular traffic, from the high use of domestic heating, as well as from the pollution produced by the industrial sector and agricultural activities located in the Po valley.

Traffic and domestic heating are among the main pollutants sources often considered responsible for poor air quality [18]. In winter, the presence of high pollutants concentrations together with few rainfalls and frequent thermal inversions worsen air quality [19]. Fuels such as wood and natural gas are actually used for domestic heating, while,

\* Focus Point on “Past and Present: Recent Advances in the Investigation of Ancient Materials by Means of Scientific Instrumental Techniques” edited by M. Aceto, C. Grifa, C. Lubritto.

<sup>a</sup> e-mail: [valeria.comite@unimi.it](mailto:valeria.comite@unimi.it) (corresponding author)

in the past decades, oil-based combustion systems, responsible for high SO<sub>2</sub> emissions, were used. At present SO<sub>2</sub> emissions in Milan are considerably decreased but some sources are still present [20]. NO<sub>x</sub> emissions are caused by traffic for 68%, domestic heating for 12%, industries for 9% and incinerators for 2%. Anthropogenic VOC emissions in urban areas are caused by the use of solvents for about 61% and by traffic for 12%. Finally, NH<sub>3</sub> emissions on a regional scale are due to agriculture and breeding activities (INEMAR, INventario EMissioni ARia, ARPA Lombardia 2014).

In urban environments the main stone surfaces degradation mechanism is sulfation and black crusts are the result of the interaction between calcium carbonate and SO<sub>2</sub>, which reacting with humidity, forms H<sub>2</sub>SO<sub>4</sub> which leads to the formation of gypsum (CaSO<sub>4</sub>·2H<sub>2</sub>O) which is the main constituent of the black crusts. It is characterized by a microcrystalline or acicular crystal structure with growth perpendicular to the degradation surface.

The analysis of black crusts has shown that, in order of abundance, carbon is the second element of anthropogenic origin, after sulfur, to be contained in the degradation layers. Its analysis makes it possible to identify pollution sources that cause BCs formation and allows to evaluate which type of pollutants are involved in the crusts formation [21,22]. In order to avoid or limiting BCs formation and to prevent surfaces degradation, some studies have been carried out with the aim to formulate new protective coatings [23,24].

The carbonaceous component of black crusts originates from PM and as a consequence the same definition has been adopted: Total carbon (TC) is composed by CC + NCC, where NCC = OC + EC; CC is the carbonate carbon which derives mainly from the substrate or deposition of soil dust, and NCC is non-carbonatic carbon, originating from anthropogenic depositions. NCC is composed of organic carbon (OC), generally of natural or anthropogenic origin [25–27], and of elemental carbon (EC), also known as BC (black carbon) because of its characteristic colour [28] and generated from combustion processes [27–29]. Furthermore the content of NCC in the black crusts is the result not only of the depositions of carbonaceous particles, but also of the adsorption of volatile organic compounds.

The determination of OC and EC and of OC/EC ratio is important to determine the type of anthropogenic depositions.

The purpose of this work is to analyse black crusts coming from the facade of the Church of Santa Maria delle Grazie al Naviglio Grande in Milan, in order to study their chemical composition and in particular the carbonaceous fractions (EC and OC) deposited and embedded within the black crusts.

Chemical characterization has been carried out both on crusts and substrates, *i.e.* bricks and mortars. From this point of view this church represents an interesting case study for the scientific community since while the process of BCs formation on natural stones (such as marbles or calcarenite) is well known, on the contrary, the study of the formation process on mortars and bricks is less common. In particular, to our knowledge, this is the first study on black crusts formed on bricks. Samples were examined by means of infrared spectroscopy (FT-IR) to detect the main mineralogical phases. Carbon, hydrogen and nitrogen (CHN) analysis and thermogravimetric analysis (TGA) were applied in order to quantify OC and EC and, finally, ion chromatography (IC) to highlight the presence of soluble salts within the crusts. The objectives of this work were: obtain information on the formation processes of BCs; understand the interaction between the substrate and the surrounding environment; identify the pollution sources responsible for the deterioration of the monument surfaces over time.

## 2 Material and methods

### 2.1 Sampling

The church of Santa Maria delle Grazie al Naviglio Grande (fig. 1) is located along the waterway Naviglio Grande nearby Milano city center in an area highly affected by traffic about 300 meters from the confluence of Naviglio in the Darsena. At present the road on which it faces is closed to traffic. The church was built at the beginning of the last century, on the remains of an earlier chapel dedicated to the Madonna delle Grazie dating back to the 16th century. The construction of the new church began in 1901, however, only the interior was completed, leaving the façade unfinished.

This new church was built in bricks and mortars, the latter includes siliceous aggregates (quartz, feldspars and micas) and aluminum-rich cement (gehlenite, alite, calcium aluminates) as attested by some art historians [30].

Overall 9 black crusts samples were taken from the facade of the church near the two aisles portals in sheltered areas, in June 2017. The samples have been collected using a scalpel and belong to three different typologies: 2 powder samples (SMN7 and SMN9 taken from brick surfaces), 3 samples of crust on brick substrate (SMN1, SMN3, SMN5) and 4 samples of crust on mortar substrate (SMN2, SMN4, SMN6, SMN8). A list of examined samples, along with their description, location, height and surface orientation, is reported in table 1. From a macroscopic point of view sampled black crusts (fig. 1) show variable morphology and thickness, depending on their exposure to deposition time. It is worth noting that since previous restoration operations have never been carried out on the church façade, the crusts represent an accumulation of about a century's pollutants.

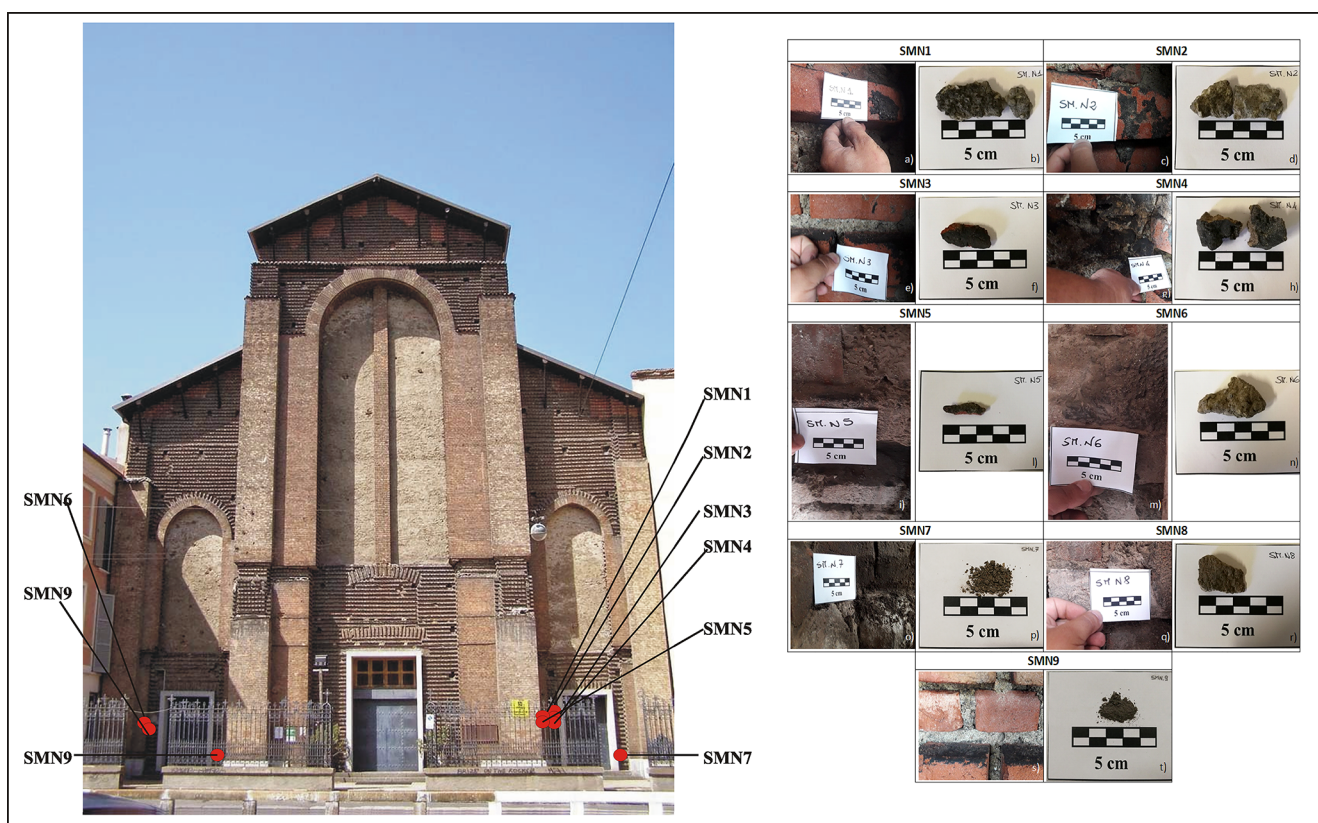


**Fig. 1.** Sampling points and pictures of the black crusts collected from the Church of Santa Maria delle Grazie al Naviglio Grande (Milan).

**Table 1.** List of samples collected from the Church of Santa Maria delle Grazie al Naviglio Grande (Milan): BC = black crust; P = powder; BR = brick substrate; M = mortar substrate.

Sample	Description	Height (cm) and sampling location	Surface orientation
SMN1	Black Crust (BC) + Brick Substrate (BR)	150 - left aisle portal	Horizontal
SMN2	Black Crust (BC) + Mortar Substrate (M)	150 - left aisle portal	Vertical
SMN3	Black Crust (BC) + Brick Substrate (BR)	150 - left aisle portal	Horizontal
SMN4	Black Crust (BC) + Mortar Substrate (M)	150 - left aisle portal	Vertical
SMN5	Black Crust (BC) + Brick Substrate (BR)	150 - left aisle portal	Horizontal
SMN6	Black Crust (BC) + Mortar Substrate (M)	150 - right aisle portal	Vertical
SMN7	Powder (P) taken from brick surfaces	100 - left aisle portal	Horizontal
SMN8	Black Crust (BC) + Mortar Substrate (M)	100 - right aisle portal	Vertical
SMN9	Powder (P) taken from brick surfaces	100 - right aisle portal	Horizontal

## 2.2 Analytical methods

For a complete characterization of BCs and of the different substrate, a multi-analytical approach, including complementary techniques, was used. Infrared spectra were collected with a spectrophotometer Nicolet 380 (Thermo Electron Corporation) coupled with ATR accessory Smart Orbit equipped with a diamond crystal. The spectra have been acquired in the range 500–4000  $\text{cm}^{-1}$  at a resolution of 4  $\text{cm}^{-1}$ . To quantify the carbonaceous components, two methodologies have been used: 1) CHN (carbon, nitrogen, hydrogen) were performed by a CHN analyser (CHNS/O Perkin Elmer 2400 Series II Elemental Analyzer using an accessory for the analysis of solids); 2) TGA (Thermo-Gravimetric) analyses were carried out by a Mettler Toledo TGA/DSC 3+ instrument which allows simultaneous TG

and DSC analyses. The analyses were conducted in the range 30–800 °C increasing the temperature with a rate of 20 °C/minute, both in oxidizing and inert atmosphere. All the calculations performed for the determination of the different fractions are reported in a previous work by La Russa *et al.* [22]; for the substrates TGA analyses were carried out only in an inert atmosphere. IC has been employed for the quantification of the main ionic species [14, 21]. Measurements of cationic ( $\text{Na}^+$ ,  $\text{K}^+$ ,  $\text{Ca}^{2+}$  and  $\text{Mg}^{2+}$ ) and anionic ( $\text{NO}_2^-$ ,  $\text{NO}_3^-$ ,  $\text{SO}_4^{2-}$  and  $\text{Cl}^-$ ) species were carried out by using an ICS-1000 HPLC system equipped with a conductivity system detector. More details on the analytical procedure are reported in Piazzalunga [31].

### 3 Results and discussion

#### 3.1 Infrared spectroscopy analysis

Regarding the mineralogical composition of analysed damage layers (BC and P), the infrared spectra (fig. 2 (a), (c), (e)) of all samples (except for the powder sample SMN7P and SMN9P) show the same absorption peaks due to calcium carbonate at 1420 and 871  $\text{cm}^{-1}$  (except for the two powder samples). This mineralogical phase has also been identified in all the mortar substrates (M) as far as concerns bricks samples, calcium carbonate was detected only in SMN1. Furthermore, in all the damage layers the characteristic absorption peaks of gypsum, at 1109, 667 and 596  $\text{cm}^{-1}$  have been identified except for samples SMN7P. The presence of a lower gypsum amount in sample SMN9 could indicate that a sulfation process leading to black crusts formation is occurring. In the substrate the presence of gypsum has not been highlighted. It is also worth to note that for the substrates very low quantity of sulphate has been identified by IC analysis (see sect. 3.3). Silicates signals at about 1000  $\text{cm}^{-1}$  are present in all the substrates. The bands of calcium oxalate, with distinctive peaks at 1630 and 1320 and 780  $\text{cm}^{-1}$ , have been revealed in all crust samples (except for the powder sample SMN7). The presence of oxalate within black crusts has been widely discussed in the scientific community [32]. In the literature the occurrence of calcium oxalate is generally due to the partial oxidation of organic carbon [33,34] ascribable to the degradation of organic protective products applied during previous restoration work, to biological activity, or to pollutants [10,35,36]. In our study the first hypothesis can be excluded since the facade of the church has never been restored. As regards the two powder samples (SMN7 and SMN9) the IR spectra are completely different indicating that in the case of sample SMN9 a sulfation process has probably started.

#### 3.2 Carbonaceous fraction (OC and EC) in the black crusts

The identification and evaluation of the carbonaceous species constituting the non-carbonate fraction of total carbon in the damage layers, particularly in urban areas, are required in order to obtain information on the possible pollutant sources [37–40] in order and to adopt mitigation measurements (such as façade cleaning operation or reduction of local vehicular traffic) to fulfil a better conservation of the stone surfaces. OC and EC are present in the black-crusts together with metal oxides that can catalyse the oxidation of  $\text{SO}_2$  promoting the formation of the crust itself [9,12]. In particular EC gives to the black crusts their characteristic aspect. In urban environments it is emitted by combustion processes, such as traffic and biomass burning [27–29,41] and is the main responsible for the soiling of monuments surfaces [42,43]. OC is also emitted by combustion processes and is both of primary, that means directly emitted, or secondary origin, *i.e.*, formed in the atmosphere because of different kind of reactions starting from the volatile organic precursors, *i.e.* VOC, volatile organic compounds [25,26].

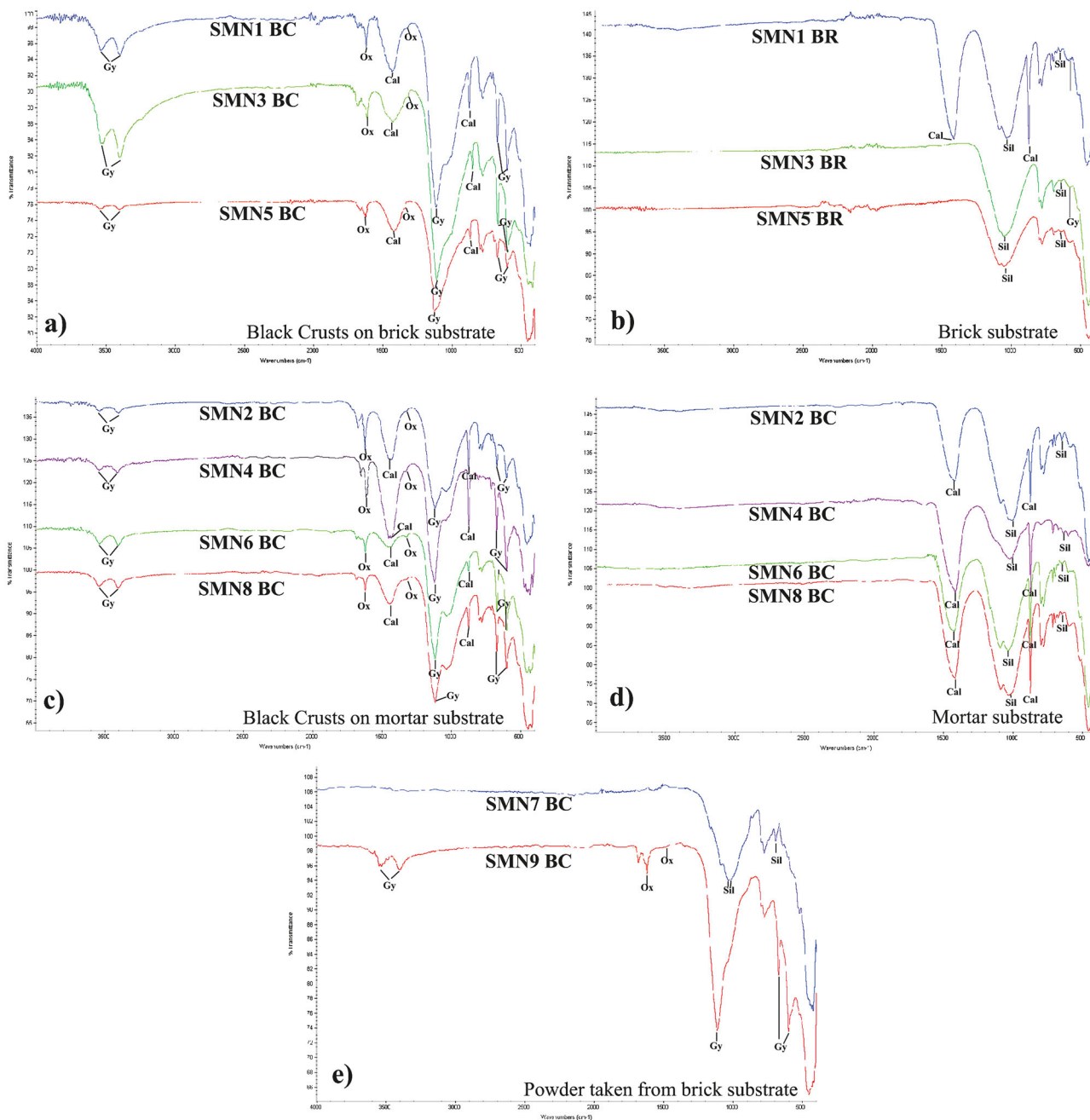
TC, OC and EC concentrations are reported in table 2. The values obtained are similar to those obtained from samples collected in other urban areas [2] with higher EC values with respect to OC [21,42] in contrast with what happens in the aerosol PM collected in the Milan area where OC is the main constituent of TC [21,44–46].

In table 2 OC/EC, EC/TC and CC (in the case of substrates) have been obtained by TGA. Elemental Carbon (EC%) and Carbonate Carbon (CC%) for BCs samples have been calculated.

The obtained OC/EC ratios are included in the range 0.18–6.75. In Milan during wintertime OC/EC ratios in PM samples generally range from 4.5 to 8.2 indicating the presence of secondary organic compounds; on the contrary values below 2–2.5, are attributable to emissions of primary pollutants [42].

In our study, it is evident how in most of the cases the crusts formation has been influenced by direct emissions such as vehicular traffic or domestic heating. In the crusts EC is preferentially embedded into gypsum. Since the facade of the church has never undergone restoration, the crusts are representative of about 100 years of accumulation of pollutants. It is also interesting to compare EC/TC ratios with those obtained in other European cities: they are perfectly in accordance with the values determined in Seville where the same ratio varies between 0.22 and 0.36 [47] indicating an analogous contribution due to traffic emissions. Also in Rome [48,49], traffic is one of the main PM sources and analogous results have been obtained [22].

$\text{TC}_{\text{CHN}}$  content in the crusts on bricks (samples SMN1, SMN3 and SMN5) is lower (table 2) being on average 1.8% for BC on bricks and 2.9% for BC on mortars. This could be due to the fact that crust formation on bricks is not favoured being CC very low, as confirmed by TGA results (table 2). BC formation process on bricks and mortars

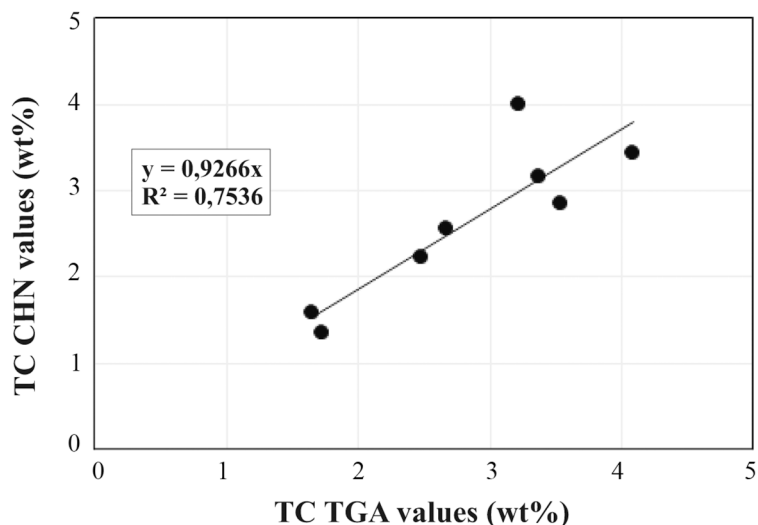


**Fig. 2.** FT-IR spectra of samples. (a) Black crusts (BC) and relative (b) BRick substrates (BR); (c) black crusts (BC) and relative (d) mortar (M) substrates; (e) powder (P) of black crusts.

substrates is different since in the case of a carbonatic substrate such as the mortar, calcium carbonate is converted into sulphate due to the reaction with sulphur dioxide while in the case of a non-carbonatic substrate such as a brick, or also a natural stone, different hypotheses have been formulated. For examples in sites interested by Saharan dust transport crusts are formed by the deposition of calcium carbonate from the atmosphere, which reacts with  $\text{SO}_2$  without a direct interaction with the substrate [50]. Another hypothesis is that some minerals present in the substrate are the source of Ca through acidic dissolution [51]. Nevertheless, it is quite interesting to observe how in the present case study average sulphate concentrations in black crusts samples taken from bricks and mortars are the same in spite of the different substrate nature ( $\text{Ca}_2\text{SO}_4 \cdot \text{H}_2\text{O}$  determined from TGA analysis is 30% and 20%, respectively, in bricks and mortars). A hypothesis is that in our case gypsum formation starting from  $\text{CaCO}_3$  present in the mortar binder is partly inhibited by the silicate aggregate. Therefore, what can be conclude is that BC formed on mortars embed a higher quantity of total carbon being sulphate concentration the same encountered in bricks.

**Table 2.** TC (total carbon); OC (organic carbon); EC (elemental carbon); CC (carbonate carbon) concentrations (wt%) for the analysed black crusts (BC) powders (P) and different substrates (BR and M).

	Black crusts and powder									Substrate	
	TC <sub>CHN</sub> %	(EC+CC) <sub>CHN</sub> %	OC <sub>CHN</sub> %	(OC/EC) <sub>TGA</sub>	(EC/TC) <sub>TGA</sub>	EC%	CC%	OX <sub>TGA</sub> %	CC <sub>TGA</sub> %		
SMN1	2.26	2.13	0.43	0.18	0.75	2.33	0.70	0.24	BR	0.59	
SMN2	3.43	2.82	0.61	0.71	0.52	0.86	1.96	0.37	M	0.91	
SMN3	1.57	0.92	0.65	0.33	0.68	1.95	0.63	0.10	BR	0.02	
SMN4	3.16	1.83	1.33	0.34	0.61	3.90	0.69	0.48	M	1.74	
SMN5	1.35	0.58	0.77	4.00	0.18	0.19	0.39	0.11	BR	0.01	
SMN6	2.84	2.12	0.71	1.40	0.41	0.51	1.61	0.03	M	1.23	
SMN8	2.22	1.61	0.62	0.64	0.55	0.98	0.63	0.20	M	1.32	
SMN7	3.99	1.51	2.47	6.75	0.31	0.37	1.14	0.15			
SMN9	2.05	1.43	0.62	1.51	0.48	0.41	1.02	0.22			
Average BC on BR substrate	1.73	1.21	0.62	1.50	0.54	1.49	0.57	0.15			
St.dev	0.47	0.81	0.17	2.16	0.31	1.14	0.16	0.08			
Average BC on M substrate	2.91	2.10	0.82	0.77	0.52	1.56	1.22	0.27			
St.dev	0.52	0.53	0.34	0.45	0.08	1.57	0.67	0.20			

**Fig. 3.** Comparison of the values of the concentrations (wt%) of the total carbon in the crusts and in the powder SMN7 obtained by analysis in TG and CHN.

A rather fair correlation between TC values obtained by CHN and TGA techniques is observable (fig. 3). While in CHN analysis TC concentrations are directly measured, TC derived from TGA have been obtained calculating OC values taking into account the conversion from OM (organic matter,  $OM = f OC$ ), that is the quantity measured by TGA from the weight loss in a specific temperature range. Sample SMN9 has been excluded from the calculation of the correlation reported in fig. 3 since the two TC values are slightly different probably because this sample was quite inhomogeneous.

From TGA oxalate concentrations (table 2) have been determined taking into account the weight loss in the same temperature range considered for a standard sample of oxalate analysed in the same conditions. The determined quantities have been confirmed by the intensity of oxalate signals in IR spectra (fig. 2): for examples in case of samples SMN4 and SMN2, characterized by the higher oxalate quantity, the peaks at  $1630$  and  $1320\text{ cm}^{-1}$  are more intense while in case of sample SMN6 are weaker, confirming the correct assignment of the weight loss due to oxalate in TGA.

**Table 3.** Concentration ppm ( $\mu\text{g/g}$ ) and average of ions in the black crusts (BC) powders (P) and different substrates (BR and M), collected from the Church of Santa Maria delle Grazie al Naviglio Grande (Milan).

		ppm ( $\mu\text{g/g}$ )							
		Na <sup>+</sup>	K <sup>+</sup>	Mg <sup>2+</sup>	Ca <sup>2+</sup>	Cl <sup>-</sup>	NO <sub>2</sub> <sup>-</sup>	NO <sub>3</sub> <sup>-</sup>	SO <sub>4</sub> <sup>2-</sup>
SMN1	BC	2141	1578	410	89889	4252	125	2088	158690
	BR	646	780	19	18282	2318	n.d.	368	9085
SMN3	BC	2176	1919	1240	90676	6576	51	52	195172
	BR	479	583	12	7321	948	481	163	8407
SMN5	BC	1128	847	528	55957	1663	26	49	114351
	BR	618	396	n.d.	1726	134	139	71	2301
BC	Average	1815	1448	726	78841	4164	67	730	156071
	St.dev	595	548	449	19822	2457	52	1177	40474
BR	Average	581	587	15	9110	1133	310	201	6597
	St.dev	90	192	4	8422	1104	242	152	3737
SMN2	BC	879	710	282	88714	2127	20	1130	94788
	M	519	752	769	57514	753	531	1026	8936
SMN4	BC	7084	6865	1863	111562	7092	22	918	189637
	M	3925	4088	279	24768	5113	186	914	37824
SMN6	BC	897	800	n.d.	100267	746	21	29	169570
	M	346	588	n.d.	49017	299	117	367	10188
SMN8	BC	927	793	752	92495	1005	92	2197	165601
	M	584	717	118	53363	552	159	1440	17714
BC	Average	2447	2292	966	98259	2743	39	1068	154899
	St.dev	1724	1703	339	14681	2297	190	442	13348
M	Average	1344	1536	388	46165	1679	248	937	18666
	St.dev	1724	1703	339	14681	2297	190	442	13348

### 3.3 Ionic chromatography analysis (IC) in the black crusts and different substrate

In table 3 and fig. 4, results regarding the determination of ionic species determined by IC, have been reported. As expected in the crusts sulphate shows the same trend of calcium, in accordance with FTIR results showing the presence of gypsum.

The two powder samples (fig. 4(e)) show different trends in accordance with what has been observed by FT-IR spectroscopy (a sulfation process is probably already started on the substrate of sample SMN9).

Sulphate concentrations have been obtained also from TGA measurements and a very fair accordance with ion chromatography results (table 3) has been observed.

In fig. 5 it the apportionment between sea salt sulphate (SS.SO<sub>4</sub>) and the non-salt sulphate (NSS.SO<sub>4</sub>) is shown in accordance with what proposed by Keene [52] and Hawley [53], and calculated using the following algorithm:  $[\text{NSS.SO}_4] = [\text{SO}_4] - (0.25 \cdot [\text{Na}])$ . As expected sulphate is mainly due to other sources, different from sea salt.

Chlorides and nitrates represent the second and the third ions in order of abundance after sulphate (figs. 3(b), (d), (e)). In the literature, nitrates and chlorides salts in mortars were mostly detected in walls higher than 50 cm confirming what observed in the present study since our samples have been collected at a high of 1.50 cm [54,55]. Furthermore, the concentrations detected in the samples from Santa Maria delle Grazie are quite similar to what

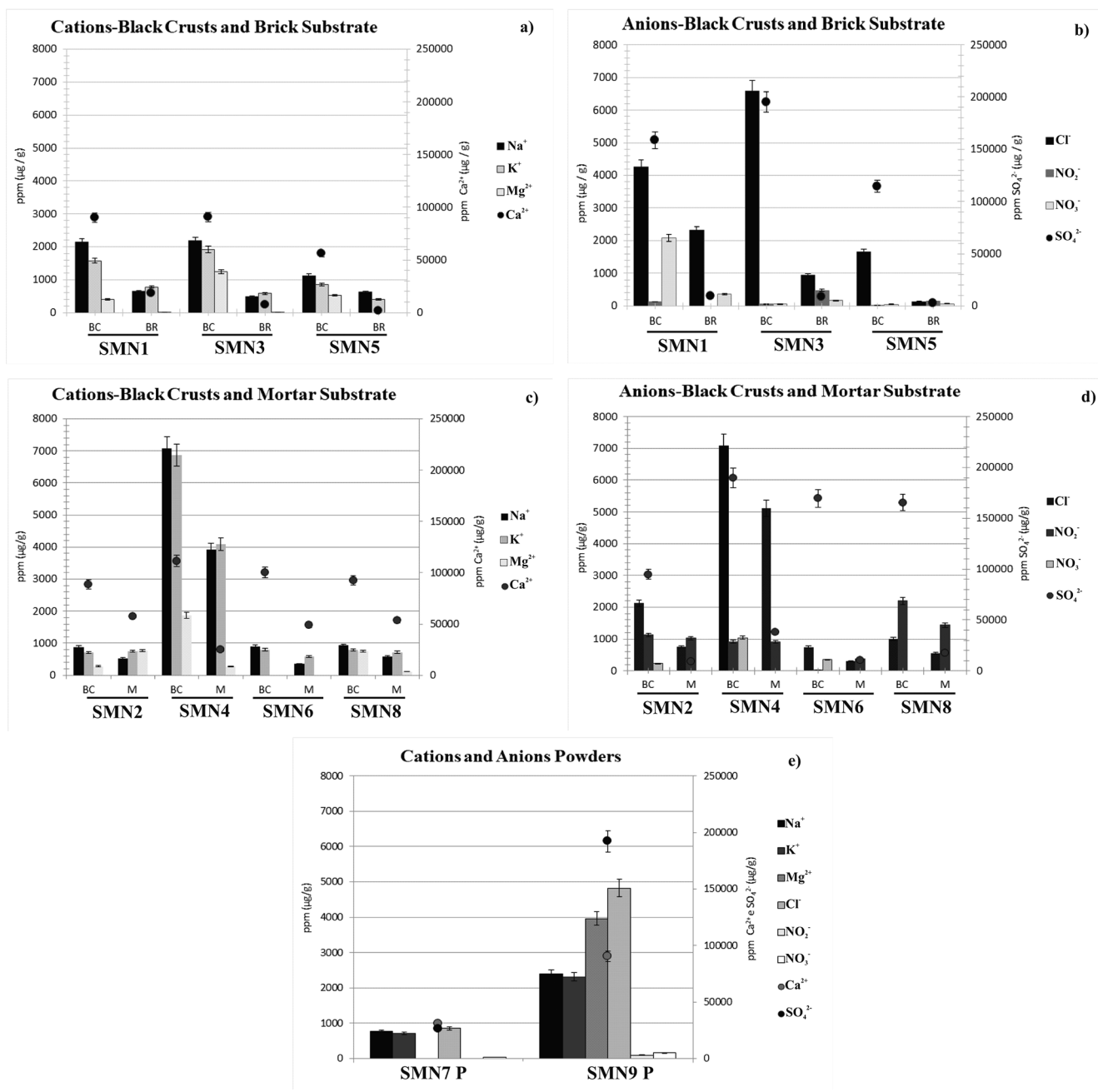


**Fig. 4.** Anions and cations concentrations ( $\mu\text{g/g}$ ) determined for the three analysed black crusts, different substrates and powder.

reported in the literature for mortars [55]. Comparing chlorides in BCs samples with the corresponding substrates it can be observed how  $\text{Cl}^-$  accumulates in the damaged layers. In fact the presence of chlorides in the analyzed samples could be attributed to two different causes: a) ascent of water by capillarity and this could be their origin since the church is located along the canal Naviglio Grande and some water infiltration could append; b) the use of not purified common salt ( $\text{NaCl}$  with a small percentages of  $\text{KCl}$  and  $\text{MgCl}_2$ ) to minimize the effects of snow and ice [55], the use of which in the cities of city of Milan is common during the winter period.

Finally we did not observe differences among samples in dependence of their orientation (horizontal or vertical, see table 1). Such differences are generally observable in the case of natural stone (higher accumulation phenomenon on horizontal surfaces) but in the present case probably the high porosity of the materials did not allow to observe any difference.

As regards potassium, which on average is higher in the crust with respect to the substrate, it could be also linked to other sources such as biomass burning [31, 56, 57].



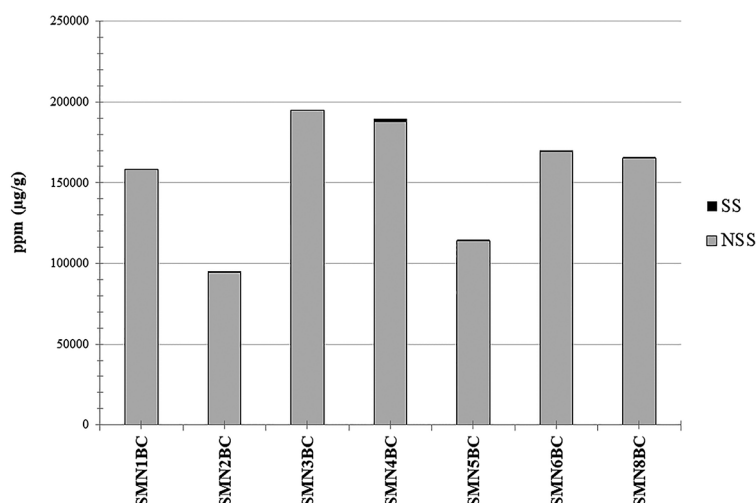


**Fig. 5.** Histograms showing the sulphate concentrations subdivided in sea salt sulphate (SS\_ $\text{SO}_4$ ) and the non-sea salt sulphate (NSS\_ $\text{SO}_4$ ), the black crusts samples.

## Conclusion

Aim of this research was the characterization and quantification of the various components present in the black crusts that due to atmospheric pollution have developed on bricks and mortars of the façade of the church of Santa Maria delle Grazie at the Naviglio Grande in Milan. The crusts sampled were subjected to a series of analyses (FT-IR spectroscopy, CHN elemental analysis, Thermal-analysis and Ion chromatography) that have allowed a complete characterization in order to obtain useful information on their formation processes.

Results indicated that the crusts are mainly composed by gypsum with lower content of calcite and oxalate.

The analysis of the main ions has confirmed the presence of large amounts of sulphate ascribable to anthropogenic sources. A high chloride concentration has been evidenced in mortar samples and it has been hypothesized that this could be due to the presence of the nearby waterway Naviglio Grande.

An in depth study has been carried out on the carbonaceous fraction (*i.e.*, organic and elemental carbon), since it is the main cause of blackening of architectural surfaces and subsequently of black crusts formation. Comparing the values obtain for black crusts with those typical of aerosol PM it is possible to get information on the contribution of the different pollution sources especially in urban areas. As regards the carbonaceous species it has been demonstrated that there is a preferential accumulation of elemental carbon even if, depending on the sample, organic substances, probably of secondary origin, can also be present. The accumulation of polluting substances of primary origin (emitted from vehicular traffic and domestic heating), was the main cause of the formation of these degradation layers on the surfaces, representing a real risk for the monuments.

It has been also observed that the deposition geometry (horizontal and vertical) in this study has not shown significant differences in terms of concentration of the analysed species probably because the porosity of the materials.

The authors acknowledge Ufficio per la Soprintendenza dei Beni Culturali della Diocesi di Milano and in particular Arch. Capponi and Arch. Lazzaroni.

## References

1. P. Brimblecombe, *Urban Air Pollution—European Aspects*, edited by J. Finger, O. Herter, F. Palmer (Kluwer, Dordrecht, 1999).
2. Sabbioni, *The Effect of Air pollution on the Built Environment* (Imperial College Press, Singapore, 2003).
3. G.G. Amoroso, V. Fassina, *Stone Decay and Conservation*, Vol. 11 (Elsevier, Amsterdam, 1983) 453.
4. D. Camuffo, M. Del Monte, C. Sabbioni, *Water Air Soil. Pollut.* **19**, 351 (1983).
5. A. Moropoulou, A. Cakmak G. Biscontin, *MRS Proc.* **462**, 307 (1996).
6. Á Török *et al.*, *Environ. Earth Sci.* **63**, 675 (2011).
7. V. Comite *et al.*, in *Rendiconti Online della Società Geologica Italiana, Arcavacata di Rende 2012*, edited by S. Critelli, F. Muto, F. Perri, F.M. Petti, M. Sonnino, A. Zuccari, Vol. 21 (Società Geologica Italiana, Roma, 2012).
8. C.M. Belfiore *et al.*, *Environ. Sci. Pollut. Res.* **20**, 8848 (2013).
9. M.F. La Russa *et al.*, *Appl. Phys. A Mater. Sci. Process.* **113**, 1151 (2013).

10. D. Gulotta *et al.*, *Earth Sci.* **69**, 1085 (2013).
11. D. Barca *et al.*, *Appl. Geochem.* **48**, 122 (2014).
12. S.A. Ruffolo *et al.*, *Sci. Total Environ.* **502**, 157 (2015).
13. V. Comite *et al.*, *Constr. Build Mater.* **152**, 907 (2017).
14. M.F. La Russa *et al.*, *Eur. Phys. J. Plus* **133**, 370 (2018).
15. Farkas *et al.*, *Environ. Earth Sci.* **77**, 211 (2018).
16. P. Fermo *et al.*, *Geosciences* **349**, 8 (2018).
17. Decreto Legislativo 13 agosto 2010, n. 155, *Attuazione della direttiva 2008/50/CE relativa alla qualità dell'aria ambientale e per un'aria più pulita in Europa* (pubblicato nella G.U. n. 216 del 15/09/2010 – suppl. ord. N. 2017 – in vigore dal 30/09/2010).
18. EEA Report No 1/2017, *Climate change, impacts and vulnerability in Europe 2016 An indicator-based report* (European Environment Agency, Luxembourg, 2017).
19. Directive 2008/50/EC of the European Parliament and of the Council of 21 May 2008 on ambient air quality and cleaner air for Europe.
20. A. Bigi *et al.*, *Atmos. Res.* **186**, 83 (2017).
21. P. Fermo *et al.*, *Environ. Sci. Pollut. Res.* **22**, 6262 (2015).
22. M.F. La Russa *et al.*, *Sci. Tot. Environ.* **297**, 593 (2017).
23. G. Cappelletti, *Prog. Org. Coat* **78**, 511 (2015).
24. F. Pino *et al.*, *Environ. Sci. Pollut. Res.* **24**, 12608 (2017).
25. A.L. Robinson *et al.*, *Science* **315**, 1259 (2007).
26. J.L. Jimenez *et al.*, *Science* **326**, 1525 (2009).
27. D.R. Gentner *et al.*, *Proc. Natl. Acad. Sci. U.S.A.* **109**, 18318 (2012).
28. D. Massabò *et al.*, *Atmos. Environ.* **108**, 1 (2015).
29. S. Fuzzi *et al.*, *Atmos. Chem. Phys.* **6**, 2017 (2006).
30. M.T. Fiorio, *Le chiese di Milano* (Mondadori Electa, 2006).
31. A. Piazzalunga *et al.*, *Anal. Bioanal. Chem.* **405**, 1123 (2013).
32. M. Del Monte, C. Sabbioni, *Environ. Sci. Technol.* **17**, 518 (1983).
33. L. Rampazzi *et al.*, *Talanta* **63**, 966 (2005).
34. C. Sabbioni, G. Zappia, *Aerobiologia* **7**, 31 (1991).
35. G. Barone *et al.*, *Environ. Geol.* **55**, 449 (2008).
36. C.M. Belfiore *et al.*, *Appl. Phys. A* **100**, 835 (2010).
37. P. Panteliadis *et al.*, *Atmos. Meas. Techniques* **8**, 779 (2015).
38. E. Cuccia *et al.*, *Atmos. Environ.* **67**, 14 (2013).
39. J.P. Putau *et al.*, *Atmos. Environ.* **38**, 2579 (2004).
40. J.P. Putau *et al.*, *Atmos. Environ.* **44**, 1308 (2010).
41. C.A. Belis *et al.*, *Atmos. Environ.* **45**, 7266 (2011).
42. N. Ghedini *et al.*, *Environ. Sci. Technol.* **40**, 939 (2006).
43. J. Tidblad *et al.*, *Int. J. Corros.* **12**, 1 (2012).
44. P. Fermo *et al.*, *Atmos. Chem. Phys.* **6**, 255 (2006).
45. R. Vecchi *et al.*, *Environ. Monit. Assess.* **154**, 283 (2009).
46. V. Bernardoni *et al.*, *Sci. Total Environ.* **409**, 4788 (2011).
47. Saiz-Jimenez, *Proceedings of the International Workshop on Air Pollution and Cultural Heritage, Seville, Spain*, edited by C. Saiz-Jimenez (Seville, Spain, 2003).
48. C. Perrino, M. Catrambone, A. Pietrodangelo, *Environ. Int.* **34**, 621 (2008).
49. S. Sandrini *et al.*, *Atmos. Environ.* **99**, 587 (2014).
50. V. Comite, Tesi di Dottorato di Ricerca in Scienze della Terra XXVI ciclo, Università degli Studi di Catania, Dipartimento di Scienze Biologiche Geologiche e Ambientali (2013).
51. J.S. Pozo-Antonio, M.F.C. Pereira, C.S.A. Rocha, *Sci. Total Environ.* **584–585**, 291 (2017).
52. W.C. Keene *et al.*, *J. Geophys. Res.* **91**, 6647 (1986).
53. A.M.E. Hawley, J.N. Galloway, W.C. Keene, *Water Air Soil Pollut.* **42**, 87 (1988).
54. C.M. Grossi *et al.*, *Sci. Total Environ.* **409**, 2577 (2011).
55. M. Veneranda *et al.*, *J. Raman Spectrosc.* **45**, 1110 (2014).
56. A. Caseiro *et al.*, *Atmos. Environ.* **43**, 2186 (2009).
57. A. Piazzalunga *et al.*, *Int. J. Environ. Anal. Chem.* **90**, 934 (2010).